Crystallization of amorphous N-doped Ge-rich GST layers deposited on a polycrystalline GST template

Minh Anh Luong, Eloïse Rahier, Sijia Ran, Alain Claverie

Crystallization of amorphous N-doped Ge-rich GST layers deposited on a polycrystalline GST template

Minh-Anh Luong, Eloïse Rahier, Sijia Ran and Alain Claverie

CEMES-CNRS and Université de Toulouse, 29 Rue Jeanne Marvig, 31055 Toulouse, France

Abstract

We report on a detailed experimental study of the crystallization of amorphous N-doped Ge-rich GST layers (GGSTN) when in contact with a polycrystalline GST template. By combining in situ annealing in the TEM and ex situ chemical analysis, we show that, as observed in many materials, the layer in contact with the crystalline template crystallizes at a lower temperature than needed for bulk crystallization. At surprise, this characteristic is not due to the solid phase epitaxy of the GGSTN on the crystalline GST template but to a decrease of the Ge content in the GGSTN layer. Indeed, during annealing, Ge diffuses from the amorphous layer into the crystalline GST layer where it gets trapped and forms grains which grow, eventually leading to the formation of a pure crystalline Ge layer. As a result of this Ge depletion, the thermal budget necessary to drive the phase separation limiting the crystallization of the remaining GGSTN alloy is smaller.

Key words: Ge-rich GeSbTe alloys, TEM and STEM, Crystallization, Chemical redistribution

1. Introduction

Phase change materials have very different physical properties, especially optical and resistive, depending on whether they are amorphous or crystalline. Their ability to change state rapidly by applying heat pulses makes them strategic materials for information storage. In electrical phase change memories (PCM), the information bit is encoded in two distinct resistive states corresponding to the amorphous state (highly resistive) and the crystalline state (conductive) [1-5]. Reversible transitions from one state to the other are achieved by supplying an appropriate amount of direct current to a cell, thereby locally heating the material. Different phase change materials are being considered for developing PCM technology, but GeSbTe alloys offer many advantages. Among them, Germanium enriched and N-doped GST-225 alloys (Ge-rich GSTN or GGSTN) are of considerable interest due to their high crystallization temperatures (>300°C) and improved characteristics suitable for embedded digital devices [6-11].

Still, the factor limiting the rate of data transfer between GGSTN phase-change memories is the writing (SET) operation, where the active material re-crystallizes from an amorphous dome surrounded by a polycrystalline matrix [12]. It is therefore essential to understand the recrystallization mechanism that operates within such cells. Whether it is obtained through the nucleation of nuclei within the amorphous dome (homogeneous crystallization) or by the growth of pre-existing crystalline grains sitting at the periphery of the dome (heterogeneous crystallization) is unknown. The answer to this question has major technological implications, regarding the optimization of writing speed and energy consumption, but also in terms of size reduction. Homogeneous nucleation leads to slower SET writing times, but these are independent of dome size. In contrast, heterogeneous crystallization from the edges of the dome will be faster, but the writing time will depend on the size of the dome.

Bulk GGST alloys crystallize homogeneously through the formation of two crystalline phases, Ge cubic and GST cubic [13,14]. In a GGSTN cell after RESET, the periphery of the dome thus consists of a mixture of fine Ge and GST grains in contact with the amorphous phase [12]. To evidence whether these grains could trigger the heterogeneous crystallization of the amorphous dome, we have studied, on full sheet layers, the effect of a crystalline GST layer on the thermal crystallization of an amorphous GGSTN layer.

2. Experimental

GST/GGSTN stacks of different thicknesses were fabricated. First, a poly-crystalline GST-225 layer (10 to 100 nm-thick) was deposited by physical vapor deposition (PVD), using a mixture of Ar and N_2 in an industrial tool, on naturally oxidized Si wafers at about 200°C. Then, an amorphous GGSTN layer (90 to 500 nm-thick) was deposited at room temperature on top of the crystalline GST layer. The Ge concentration (in atomic fraction) in the GGSTN layer was above 50% while the N content was above 5%. The stack was protected against oxidation by a 20 nm-thick TiN capping layer.

Ex situ annealing experiments were conducted in a horizontal Carbolite furnace under atmospheric pressure and N_2 gas flow for temperatures ranging from 310 to 400 °C and times from 30 min to 81 h. Cross-sectional samples for TEM analyses were prepared by focus ion beam (FIB) using an FEI Helios NanoLab 600 (FEI Company) operating with a 30 keV Ga ion beam and finally polished and cleaned at 2 keV. In parallel, the real time observation of the thermal crystallization of the film was observed *in situ* in a TEM, in bright-field (BF) and dark-field (DF) imaging modes. These *in situ* heating experiments were performed using a Gatan 652 double tilt heating specimen holder. During the *in situ* heating, the temperature was increased by steps of 10 °C from about 200 °C, using a ramping rate of 1 °C/s, and held for 5 min at each temperature during which the sample was imaged by TEM.

The samples were imaged and analyzed using various TEM machines, an aberration-corrected FEI TECNAI F20 (200 KeV) for high resolution (HR) TEM imaging, a Philips CM20-FEG (200 KeV) equipped with a Microanalyzer QUANTAX XFlash detector (with a 30 mm^2 active area providing an energy resolution of 127 eV) for Energy-dispersive X-ray spectroscopy (EDX) mapping, and a probe corrected ARM JEM JEOL 200F microscope (200 kV) for high-angle annular dark-field (HAADF)-STEM imaging and Electron Energy Loss Spectroscopy (EELS) analysis. The EDX maps were obtained by scanning the probe on a 2D raster with a step size of about 2-3nm. To increase the quantification precision, the acquisition time for each spectrum was maintained for about 30 min with an X-ray counting rate of about 4 kcps. Data acquisition and quantitative analyses were performed using Esprit 1.9 software from Bruker, employing the "Cliff and Lorimer ratio method", with an absolute uncertainty of about 3% (molar fraction). The elemental maps and compositional ratios of Ge, Sb, and Te were extracted using Ge- K, Sb- (K, L) and Te- (K, L) energy levels. Electron Energy-Loss Spectroscopy (EELS) spectra were acquired with a convergence semi-angle of 14.8 mrad and a spectrometer collection semi-angle of 19.4 mrad. The spectrum images were acquired in dual EELS mode with the entrance GIF aperture of 2.5mm and an energy dispersion of 0.5 eV, giving an energy resolution of 1.5eV/channel. Prior to the TEM characterizations, a beam shower of 15 min was done on the samples to reduce contamination and sample drift during the acquisition. Data processing was performed using the Gatan Digital Micrograph software.

3. Results and discussion

Sample description

Figure 1 shows the structure of the sample made of a 90 nm-thick GGSTN layer deposited on top of a 10 nm-thick crystalline GST. The TEM images and selected area diffraction (SAED) patterns (not shown) confirm the amorphousness of the top GGSTN layer and the crystallinity of the underlying GST layer. The Ge, Sb and Te EELS elemental maps (Fig. 1, bottom) show the two layers are chemically homogeneous and close to the targeted stoichiometry.
Moreover, it has to be noticed that, whatever their thicknesses, the GST layers are made of small grains of mostly the hexagonal GST phase, with the basal planes parallel to the wafer surface (Fig. 2). As a result of this texture, the grains are separated by grain boundaries, mostly standing perpendicular to the layer. Furthermore, local composition fluctuations result in the presence of intra-grain defects and variations in the size of the Hex-GST blocks separated by Van der Waals gaps (Fig. 2.c).

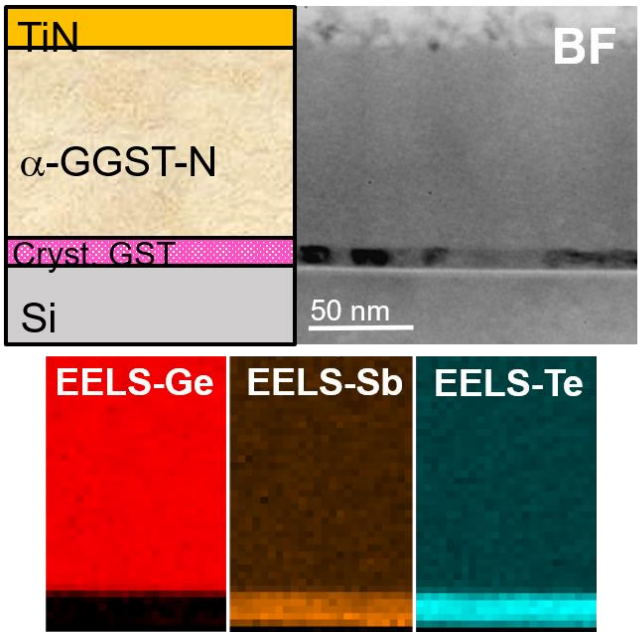

Figure 1. *Top-left figure shows a schematic demonstration of investigated structure and top-right figure shows a BF TEM image of the fabricated sample. The bottom figures show EELS maps of Ge, Sb and Te in red, orange and cyan color, respectively.*

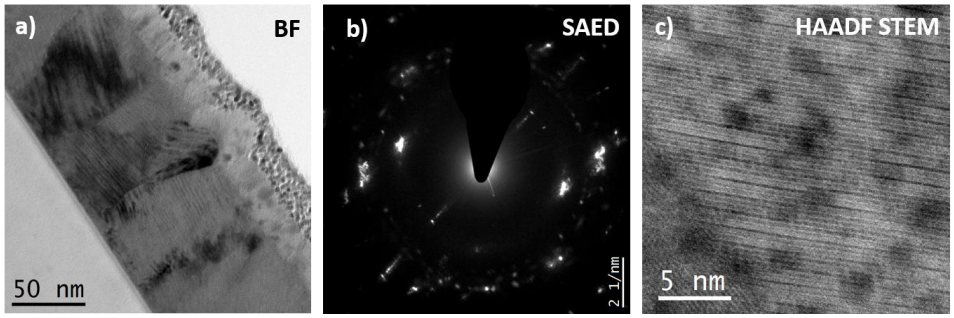

Figure 2. *TEM images of a 100 nm-thick crystalline GST layer showing the typical features characteristic of all the crystalline GST layers on which amorphous GGSTN is deposited. Grains of columnar structure and Hex-GST phase are observed (a). Stacking defects are detected by the streaks in the SAED pattern (b) and observed by HAADF (c) within the grains.*

Impact on crystallization temperature and kinetics of GGSTN

First, to evidence the impact of the crystalline GST layer on the crystallization of amorphous GGSTN, we have annealed together at 380°C for 30 min a GST/GGSTN stack and a control sample consisting of a plain GGSTN layer directly deposited onto the native silicon oxide.
Figure 3 compares the structure of these GGSTN layers after annealing at 380 °C for 30 min. While the layer deposited directly on the Si oxide (Fig. 3.a) is still amorphous, the layer deposited on the crystalline GST layer is crystalline (Fig. 3.b). The brightfield and darkfield images of the stack (Fig. 3.b top and bottom respectively) show the crystallization of small cubic Ge and bigger cubic GST grains in the GGSTN layer. Surprisingly, we do not observe any grains that have grown from the GST crystalline template or any other evidence of heterogeneous crystallization of the GGSTN material.

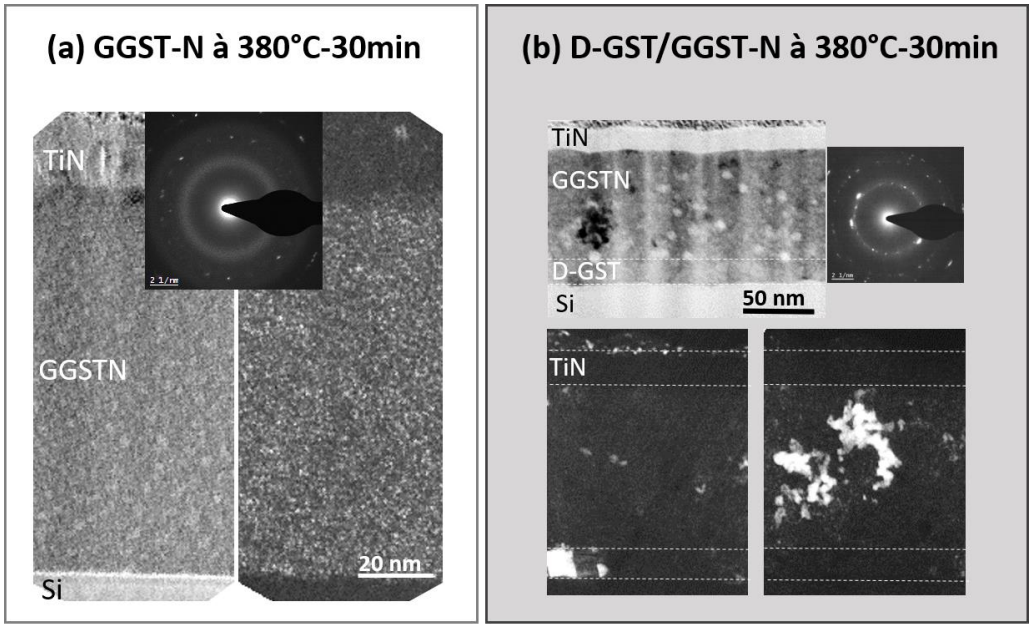

Figure 3. (a) *BF and DF TEM images taken on the control GGSTN sample, annealed at 380 °C for 30 min. The inserted SAED pattern shows the amorphousness of the deposited layer.* ***(b)*** *BF and DF TEM images of the sample "GGSTN/GST" annealed at 380 °C for 30 min. The inserted SAED pattern and DF images show the presence of FCC Ge and GST-225 crystals.*

We investigated further the crystallization mechanism of the GGSTN layers by performing *in situ* annealing in the TEM. Figure 4 shows bright and darkfield images recorded during annealing of a GST/GGSTN stack at 385°C. Small Ge crystals are progressively nucleated and randomly distributed within the layer. The crystallization mechanism of the GGSTN layer therefore remains homogeneous and unchanged from bulk GGSTN, with first the homogeneous crystallization of Ge followed by the progressive crystallization of a GST phase [15,16]. However, this crystallization takes place at a temperature significantly lower than observed in bulk GGSTN, by about 10 to 20°C, although no clear effect of the crystalline template can be evidenced [17].

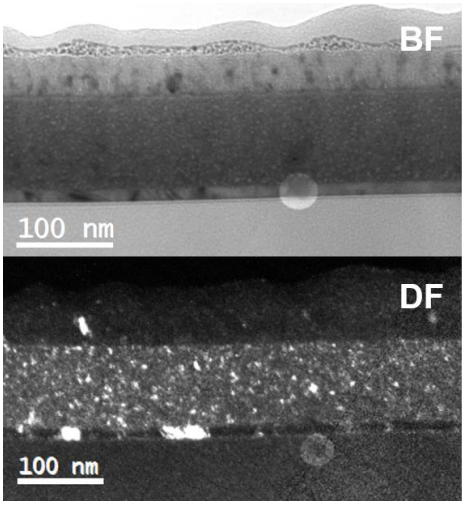

Figure 4. *BF and DF images taken during in situ annealing of the GST/GGSTN stack at 385 °C. Ge grains are seen nucleating homogeneously in the GGSTN layer with no apparent influence of the crystalline GST template.*

Chemical redistribution

To understand the origin of this lowering of the crystallization temperature, we performed chemical STEM-EELS analysis on the sample annealed at 380°C for 30 min. Figure 5 displays a set of (S)TEM images and EELS elemental maps of this sample. At surprise, the EELS maps and the HRTEM images show that the former crystalline GST layer no longer exists but has been completely replaced by a layer of pure Ge grains during annealing.

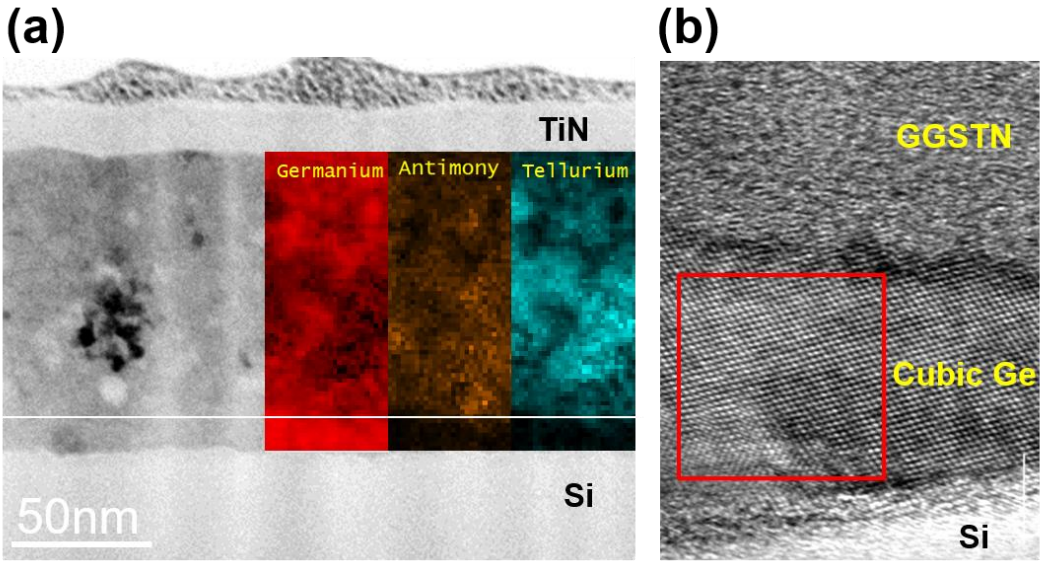

Figure 5. ***(a)*** *TEM analyses of a GGSTN/GST stack annealed at 380 °C for 30 min. EELS elemental maps are inserted on the brightfield TEM image. The thin crystalline layer is now made out of pure Ge grains.* ***(b)*** *High Resolution TEM image showing the Ge cubic lattice below the GGSTN layer, where the crystalline GST layer was located before annealing.*

To understand how thermal annealing can lead to the replacement of our GST crystalline template by a pure polycrystalline Ge layer, we studied the kinetics of this phenomenon during ex situ isothermal annealing at low temperatures and for long annealing times. Figure 6 shows the evolution of the chemical composition of a GST/GGSTN stack during annealing at 310 °C for up to 24 h. During this annealing, the Ge (Fig. 6, in red) contained in the GGSTN layer diffuses towards the GST crystalline template where it progressively accumulates. In reaction, the Sb and Te initially present in the GST diffuse towards the GGSTN layer. During the first hours, we observe a "classical" diffusion phenomenon in which the concentration gradients of the different species tend to decrease. Ge diffuses towards the crystalline layer, while Sb and Te escape from it. After 4 h of annealing, the Ge concentration “rises” and an inverse gradient is formed (“uphill diffusion”). This phenomenon is characteristic of the precipitation of a species during which this species, initially free to diffuse, is rendered immobile by the formation of a phase containing it [18]. It should be noted that this phenomenon occurs while the GGSTN layer is still amorphous, as demonstrated by the SAED pattern taken after 84 h at this temperature (Fig. 6.f). At this point, the GST layer is completely replaced by a layer of polycrystalline Ge. In parallel, the interchange of elements between the GST and the GGSTN layers have modified the initial stoichiometry of the GGSTN layer. Indeed, the thermal redistribution we evidence depletes the GGSTN in Ge and enriches it in Sb and Te. As a result, the GGSTN layer that will have to crystallize is poorer in Ge than the initial GGSTN that was deposited.

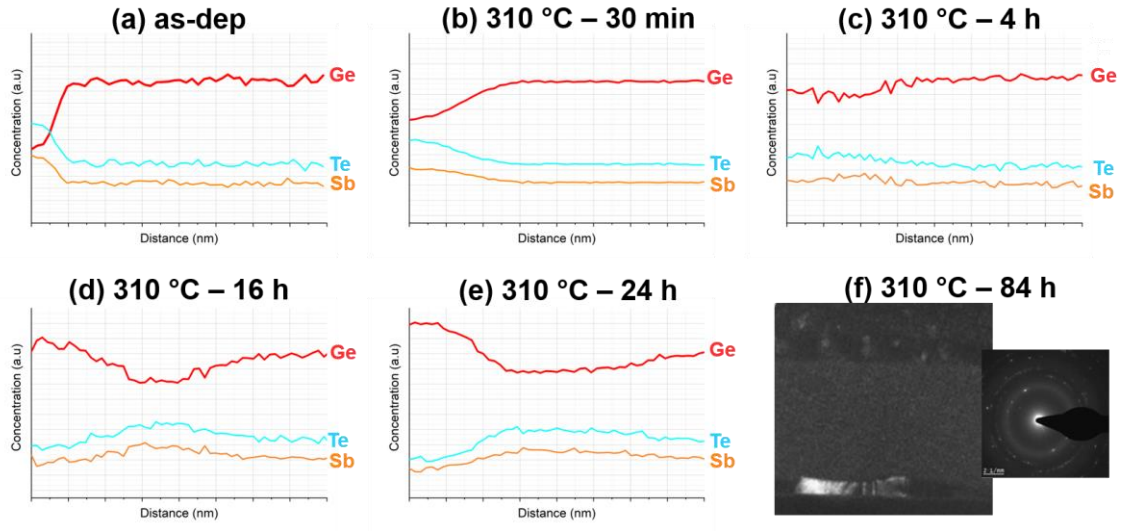

Figure 6. *Evolution of the chemical distributions of Ge (red), Sb (orange) and Te (cyan) during ex situ isothermal annealing at 310 °C of a GST/GGSTN sample* ***(a),*** *after deposition,* ***(b****), after annealing for 30 min,* ***(c),*** *4 h,* ***(d),*** *16 h and* ***(e),*** *24 h. The profiles were obtained by EDX. Y scale in arbitrary units, only to guide the eyes.* ***(f)*** *Dark field image and diffraction pattern of the same sample annealed at 310 °C for 84 h showing that the GGSTN layer is still amorphous.*

Voids formation

Another surprising feature of the material after annealing is the large number of voids found in the GGSTN layer. The presence of voids is common in GST materials [19-21]. It is generally accepted that they form during the densification phase that precedes and accompanies the crystallization of the material [22]. They are therefore generally observed after crystallization.
However, their formation during the annealing of GGSTN layers deposited on a GST template are different. The voids form while the Ge diffuses into the crystalline layer where it segregates, and the GGSTN is still amorphous. Figure 7 shows a montage of TEM images (HAADF and EELS) of a sample annealed at 360 °C for 30 minutes. The HAADF image (Fig 7.a) shows the population of voids (darkest contrast) formed after annealing. They are distributed in size, and are larger close to the interface with the crystalline layer. The STEM-EELS analysis shows that the largest voids are filled with argon. They are therefore bubbles, inserted into the amorphous GGSTN matrix, and formed by the co-precipitation of vacancies and Argon.

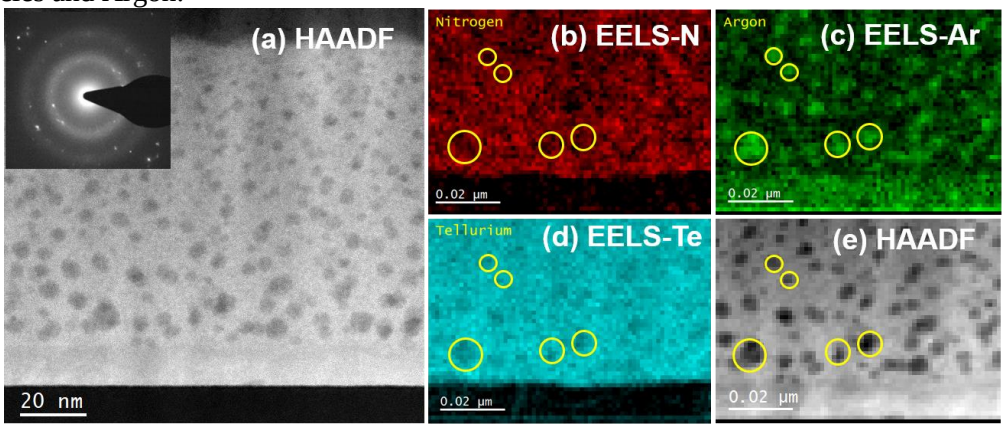

Figure 7. ***(a)*** *HAADF image and diffraction pattern of a GST/GGSTN sample annealed at 360°C for 30 min. The halo in the SAED pattern shows the GGST layer is amorphous (small spots from TiN cap layer)* ***(b), (c), (d), (e)*** *EELS maps of Nitrogen, Argon, Tellurium and corresponding*

HAADF image taken from the analyzed area. The areas of darkest contrast in HAADF (circled in yellow) correspond to the voids. The largest ones are filled with Argon.

Mechanisms and discussion

In order to study more comfortably the chemical exchanges that take place between the GGSTN amorphous layer and the crystalline GST layer during annealing, we have used thicker layers of GGSTN and GST. The mechanisms at work can be identified using a combination of HAADF images and EELS maps, as shown in figure 8, obtained after annealing at 330°C for 30 min.

In the HAADF image, Ge-rich regions appear dark. One can see that the region close to the GGSTN/GST interface becomes depleted in Ge while this Ge has obviously diffused into the GST layer, decorating the grain boundaries and segregating within some of the GST grains. EELS maps reveal that, in response, Sb and Te escape from this layer and locally enrich the GGSTN layer, close to the interface. At the same time, voids (bubbles) form, preferably at places where the Ge – (Sb, Te) exchanges have been most pronounced.

From this observation, we believe that the segregation of Ge and the replacement of the GST layer, in which there are many Van der Waals gaps between the Hex-GST blocks, by a cubic Ge phase is necessarily accompanied by a densification of the material. To achieve this, the GST layer must emit large quantities of vacancies into the GGSTN layer. These vacancies agglomerate and precipitate in the form of voids. The injection of vacancies from the crystalline layer generates a gradient in the GGSTN layer from the GST/GGSTN interface towards the GGSTN surface. It is this negative gradient that is responsible for the voids' size distribution observed in Figure 8.

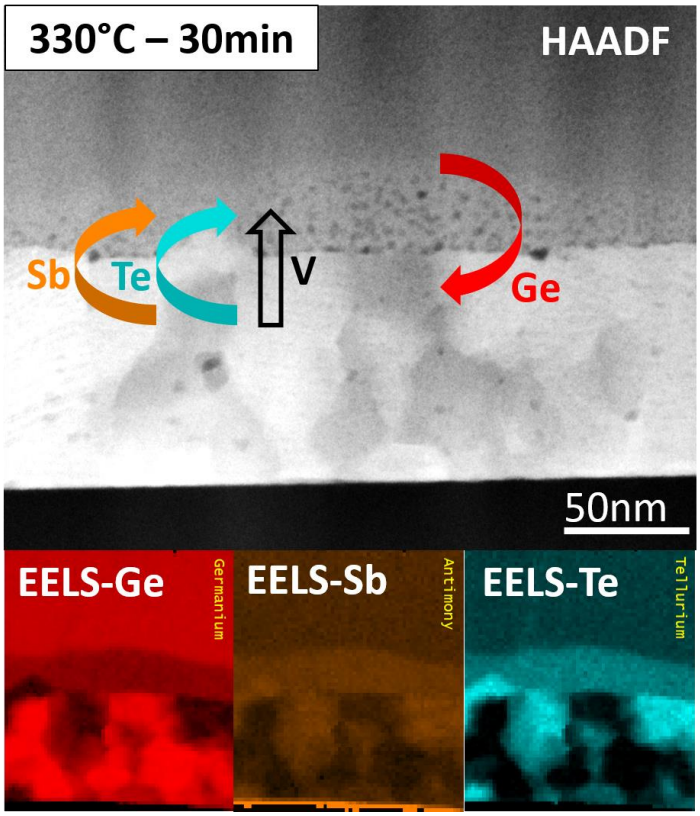

Figure 8. *HAADF image and EELS mapping of a GST/GGSTN sample annealed at 330°C for 30 min. Chemical exchanges are represented by arrows in the HAADF image.*

As already pointed out, this chemical interchange and global redistribution, occurring while the GGSTN layer is still amorphous, changes the composition of the GGSTN alloy, depleting it in Ge and enriching

it in Sb and Te, before crystallization. Since the seminal work of Zuliani et al., it has been established that the crystallization temperature of Ge-rich GST alloys increases with the Ge content of the layers [6]. This characteristic is not an intrinsic property of the alloys but reflects the need for phase separation between Ge and GST in the amorphous phase before crystallization can take place [15]. The lower the Ge content of the amorphous layer, the shorter the time required for phase separation, or the lower the temperature at which phase separation can be achieved.

We thus conclude that the crystallization of GGSTN layers observed at lower temperatures when deposited on a crystalline GST template is not due to the initiation of heterogeneous crystallization from the template, but to Ge depletion in the layer prior to crystallization.

The reduction of crystallization temperature would therefore be a secondary effect resulting primarily from the "Ge trapping capacity" of the crystalline layer. Luong et al. have established that Ge can diffuse rapidly at the grain boundaries between GST grains, much more rapidly than observed in the amorphous alloys [23]. Such diffusion paths are numerous in these GST layers and therefore they allow Ge atoms to diffuse quickly within the layer where they can segregate and rapidly crystallize by heterogeneous nucleation on these defects. This occurs before the homogeneous nucleation of any crystalline phase in the upper GGST layer is possible. Whilst the effect of the relative thicknesses of the two layers has not been formally studied in this paper, we can infer that the thicker the crystalline layer is, the higher its "Ge trapping capacity" would be, generating a GGSTN layer even more depleted in Ge, that would crystallize at a lower temperature.

4. Conclusion

Putting together all the results we have obtained, the effect of a crystalline GST template on the crystallization of an amorphous GGST-N layer during annealing can be summarized as follows. During annealing, Ge diffuses in the amorphous GGSTN and in and through the crystalline template, using mainly grain boundaries. It then starts nucleating as a Ge phase on the defects offered by the polycrystalline layer. To balance the incoming Ge, Sb and Te exodiffuse from the GST crystalline template into the GGSTN layer. The growth of the Ge phase causes a densification of the polycrystalline layer, which emits the structural vacancies contained in the GST template, in the amorphous GGSTN layer. These vacancies precipitate and form voids. Their size distribution reflects the vacancy concentration gradient in the region. As time passes, this phenomenon leads to the complete replacement of the crystalline GST template by a pure Ge polycrystalline layer and the formation of a dense population of voids in the GGSTN layer. This phenomenon occurs while the GGSTN layer is still amorphous and is then less rich in Ge than after deposition. As a result, the phase separation required to crystallize the Ge-rich alloys demands less energy and crystallization occurs at a lower temperature.

Conflicts of Interest: The authors declare no conflict of interest.

Acknowledgements:

This work is part of the "Ô-GST Project" and was partially funded by the EUR grant NanoX n° ANR-17-EURE-0009 in the framework of the « Programme des Investissements d'Avenir ».

References

[1] M. Wuttig, N. Yamada, Phase-Change Materials for Rewriteable Data Storage. *Nature Mater* **2007**, *6* (11), 824–832. https://doi.org/10.1038/nmat2009

[2] B. C. Lee, P. Zhou, J. Yang, Y. Zhang, B. Zhao, E. Ipek, O. Mutlu, D. Burger, Phase-Change Technology and the Future of Main Memory. *IEEE Micro* **2010**, *30* (1), 143–143. https://doi.org/10.1109/MM.2010.24

[3] S. Raoux, W. Wełnic, D. Ielmini, Phase Change Materials and Their Application to Nonvolatile Memories. *Chem. Rev.* **2010**, *110* (1), 240–267. https://doi.org/10.1021/cr900040x.

[4] P. Noé, C. Vallée, F. Hippert, F. Fillot, J.-Y. Raty, Phase-Change Materials for Non-Volatile Memory Devices: From Technological Challenges to Materials Science Issues. *Semicond. Sci. Technol.* **2018**, *33* (1), 013002. https://doi.org/10.1088/1361-6641/aa7c25.

[5] P. Guo, A. Sarangan, I. Agha, A Review of Germanium-Antimony-Telluride Phase Change Materials for Non-Volatile Memories and Optical Modulators. *Applied Sciences* **2019**, *9* (3), 530. https://doi.org/10.3390/app9030530.

[6] P. Zuliani, E. Varesi, E. Palumbo, M. Borghi, I. Tortorelli, D. Erbetta, G. D. Libera, N. Pessina, A. Gandolfo, C. Prelini, L. Ravazzi, R. Annunziata, Overcoming Temperature Limitations in Phase Change Memories With Optimized GexSbyTez. *IEEE Trans. Electron Devices* **2013**, *60* (12), 4020–4026. https://doi.org/10.1109/TED.2013.2285403.

[7] A. Kiouseloglou, G. Navarro, V. Sousa, A. Persico, A. Roule, A. Cabrini, G. Torelli, S. Maitrejean, G. Reimbold, B. De Salvo, F. Clermidy, L. Perniola, A Novel Programming Technique to Boost Low-Resistance State Performance in Ge-Rich GST Phase Change Memory. *IEEE Trans. Electron Devices* **2014**, *61* (5), 1246–1254. https://doi.org/10.1109/TED.2014.2310497.

[8] E. Palumbo, P. Zuliani, M. Borghi, R. Annunziata, Forming Operation in Ge-Rich GexSbyTez Phase Change Memories. *Solid-State Electronics* **2017**, *133*, 38–44. https://doi.org/10.1016/j.sse.2017.03.016.

[9] Y.-H. Lee, P. J. Liao, V. Hou, D. Heh, C.-H. Nien, W.-H. Kuo, G. T. Chen, S.-M. Yu, Y.-S. Chen, J.-Y. Wu, X. Bao, C. H. Diaz, Composition Segregation of Ge-Rich GST and Its Effect on Reliability. In ***2021** IEEE International Reliability Physics Symposium (IRPS)*; IEEE: Monterey, CA, USA, 2021; pp 1–6. https://doi.org/10.1109/IRPS46558.2021.9405168.

[10] A. Redaelli, E. Petroni, R. Annunziata, Material and Process Engineering Challenges in Ge-Rich GST for Embedded PCM. *Materials Science in Semiconductor Processing* **2022**, *137*, 106184. https://doi.org/10.1016/j.mssp.2021.106184.

[11] P. Cappelletti, R. Annunziata, F. Arnaud, F. Disegni, A. Maurelli, P. Zuliani, Phase Change Memory for Automotive Grade Embedded NVM Applications. *J. Phys. D: Appl. Phys.* **2020**, *53* (19), 193002. https://doi.org/10.1088/1361-6463/ab71aa.

[12] A. Redaelli, editor, *Phase Change Memory* **2018** (Springer International Publishing, Chap. 7)

[13] M. Agati, M. Vallet, S. Joulié, D. Benoit, and A. Claverie, Chemical Phase Segregation during the Crystallization of Ge-Rich GeSbTe Alloys, *J. Mater. Chem.* **2019,** *28 (7)*, 8720-8729. https://doi.org/10.1039/c9tc02302j

[14] S. Privitera, I. López García, C. Bongiorno, V. Sousa, M. C. Cyrille, G. Navarro, C. Sabbione, E. Carria, and E. Rimini, Crystallization Properties of Melt-Quenched Ge-Rich GeSbTe Thin Films for

Phase Change Memory Applications, *Journal of Applied Physics* **2020,** *128*, 155105. https://doi.org/10.1063/5.0023696

[15] E. Rahier, S. Ran, N. Ratel-Ramond, S. Ma, L. Calmels, S. Saha, C. Mocuta, D. Benoit, Y. Le-Friec, M.-A. Luong, and A. Claverie, Crystallization of Ge-Rich GeSbTe Alloys: The Riddle Is Solved, *ACS Applied Electronic Materials* **2022**, *4* (6), 2682-2688. https://doi.org/10.1021/acsaelm.2c00038

[16] M. Agati, F. Renaud, D. Benoit, A. Claverie, In-situ transmission electron microscopy studies of the crystallization of N-doped Ge-rich GeSbTe materials, *MRS Communications* **2018**, *8*, 1145–1152 https://doi.org/10.1557/mrc.2018.168

[17] M.-A. Luong, D. Wen, E. Rahier, N. Ratel Ramond, B. Pecassou, Y. Le Friec, D. Benoit, A. Claverie, Impact of Nitrogen on the Crystallization and Microstructure of Ge-Rich GeSbTe Alloys, *Phys. Status Solidi RRL* **2020,** *15* (3), 2000443. https://doi.org/10.1002/pssr.202000443

[18] S. Personnic, K. K. Bourdelle, F. Letertre, A. Tauzin, N. Cherkashin, A. Claverie, R. Fortunier, and H. Klocker, Impact of the Transient Formation of Molecular Hydrogen on the Microcrack Nucleation and Evolution in H-Implanted Si (001), *Journal of Applied Physics* **2008**, *103*, 023508. https://doi.org/10.1063/1.2829807

[19] K. Do, D. Lee, D.-H. Ko, H. Sohn, M.-H. Cho, TEM Study on Volume Changes and Void Formation in $Ge_2Sb_2Te_5$ Films, with Repeated Phase Changes. Electrochem. *Solid-State Lett*. **2010**, *13* (8). https://doi.org/10.1149/1.3439647

[20] G.W. Burr, M.J. Breitwisch, M. Franceschini, D. Garetto, K. Gopalakrishnan, B. Jackson, B. Kurdi, C. Lam, L.A. Lastras, A. Padilla, B. Rajendran, S. Raoux, R. S. Shenoy, Phase change memory technology, *J. Vac. Sci. Technol. Nanotechn. Microelectr.: Mater. Proces. Measure. Phenom*. **2010,** *28* (2), 223–262. https://doi.org/10.1116/1.3301579

[21] S. H. Oh, K. Baek, S. K. Son, K. Song, J. W. Oh, S.-J. Jeon, W. Kim, J. H. Yoo, K. J. Lee, In Situ TEM Observation of Void Formation and Migration in Phase Change Memory Devices with Confined Nanoscale Ge2Sb2Te5. *Nanoscale Adv.* **2020**, *2* (9), 3841–3848. https://doi.org/10.1039/D0NA00223B

[22] L. Krusin-Elbaum, C. Cabral, K. N. Chen, M. Copel, D. W. Abraham, K. B. Reuter, S. M. Rossnagel, J. Bruley, V. R. Deline, Evidence for Segregation of Te in Ge2Sb2Te5 Films: Effect on the "Phase-Change", *Stress. Applied Physics Letter* **2007**, *90* (14), 141902. https://doi.org/10.1063/1.2719148

[23] M.-A. Luong, S. Ran, M. Bernard, and A. Claverie, An Experimental Study of Ge Diffusion through Ge2Sb2Te5, *Materials Science in Semiconductor Processing* **2022**, *152*, 107101. https://doi.org/10.1016/j.mssp.2022.107101